Proposal for an Optical Test of the Einstein Equivalence Principle

Daniel R. Terno,[1, *] Francesco Vedovato,[2] Matteo Schiavon,[2] Alexander R. H. Smith,[3]
Piergiovanni Magnani,[4] Giuseppe Vallone,[2] and Paolo Villoresi[2, †]

[1]*Department of Physics and Astronomy, Macquarie University, Sydney NSW 2109, Australia*
[2]*Dipartimento di Ingegneria dell'Informazione, Università degli Studi di Padova, Padova 35131, Italy*
[3]*Department of Physics and Astronomy, Dartmouth College, Hanover, New Hampshire 03755, USA*
[4]*Department of Physics, Politecnico di Milano, Milano 20133, Italy*
(Dated: November 13, 2018)

The Einstein Equivalence Principle (EEP) underpins all metric theories of gravity. Its key element is the local position invariance of non-gravitational experiments, which entails the gravitational red-shift. Precision measurements of the gravitational red-shift tightly bound violations of the EEP only in the fermionic sector of the Standard Model, however recent developments of satellite optical technologies allow for its investigation in the electromagnetic sector. Proposals exploiting light interferometry traditionally suffer from the first-order Doppler effect, which dominates the weak gravitational signal necessary to test the EEP, making them unfeasible. Here, we propose a novel scheme to test the EEP, which is based on a double large-distance optical interferometric measurement. By manipulating the phase-shifts detected at two locations at different gravitational potentials it is possible to cancel-out the first-order Doppler effect and observe the gravitational red-shift implied by the EEP. We present the detailed analysis of the proposal within the post-Newtonian framework and the simulations of the expected signals obtained by using two realistic satellite orbits. Our proposal to overcome the first-order Doppler effect in optical EEP tests is feasible with current technology.

Introduction.—The Einstein equivalence principle (EEP) is the foundation of all metric theories of gravity, including general relativity [1–3]. The principle is comprised from three statements. The first, known as the *weak equivalence principle*, states that the trajectory of a freely falling test body is independent of its internal structure and composition. The two other statements deal with outcomes of non-gravitational experiments that are performed in freely falling laboratories where self-gravitational effects are negligible. The second statement — *Local Lorentz Invariance* — asserts that such experiments are independent of the velocity of the laboratory where the experiment takes place. The third statement — *Local Position Invariance* (LPI) — asserts that "the outcome of any local non-gravitational experiment is independent of where and when in the universe it is performed" [1].

Tests of the "when" part of the EEP bound the variability of the non-gravitational constants over cosmological time scales [4, 5]. The "where" part was expressed in Einstein's analysis [6] of what in modern terms is a comparison of two identical frequency standards in two different locations in a static gravitational field. In fact, the so-called *red-shift* implied by the EEP affects the locally measured frequencies of a spectral line that is emitted at location 1 with ω_1 and then detected at location 2 with ω_2. The red-shift can be parametrized as

$$\frac{\Delta\omega}{\omega_1} = (1+\alpha)(U_2 - U_1) + \mathcal{O}(c^{-3}) \qquad (1)$$

where $\Delta\omega := \omega_2 - \omega_1$, $U_i := -\phi_i/c^2$ has the opposite sign of the Newtonian gravitational potential ϕ_i at the emission (1) and detection (2), while $\alpha \neq 0$ accounts for possible violations of LPI. In principle, α may depend on the nature of the clock that is used to measure the red-shift [1]. The standard model extension (SME) includes all possible

Lorentz- and CPT-violating terms that still preserve the fundamental $SU(3) \times SU(2) \times U(1)$ gauge invariance and power-counting renormalizability [7]. The SME contains variously constrained parameters whose different combinations may lead to $\alpha \neq 0$ [8–10]. A variety of alternative theories of gravity that are not ruled out by current data also predict nonzero values of α [1, 11].

A typical red-shift experiment involves a pair of clocks, naturally occurring [12] or specially-designed [13–16], whose readings are communicated by electromagnetic (EM) radiation. Recently, the comparison of co-located ultra-precise clocks, which use two different atoms (hydrogen and cesium) for their working transitions, allowed for a bound to be placed on the difference $\alpha_H - \alpha_{Cs}$ with high precision [16]. On the other hand, this estimation of α is based on implicit or explicit assumptions on the standard propagation of the EM radiation [10]. Hence, different types of experiments which employ that use a single EM-source and compare optical phase differences between beams of light traversing different paths in a gravitational field provide a complementary test of LPI.

As an example, the "optical" Colella-Overhauser-Werner (COW) experiment [17] was proposed in [18] and suggested in [19] as a possible scientific component of the QEYSSAT mission. A photon time-bin superposition [20] is sent from a ground station on Earth to a spacecraft, both equipped with an interferometer of imbalance l, in order to temporally recombine the two time-bins and obtain an interference pattern depending on the gravitational phase-shift [19],

$$\varphi_{gr} = \frac{\Delta\omega}{\omega}\frac{2\pi}{\lambda}l \approx (1+\alpha)\frac{2\pi}{\lambda}\frac{ghl}{c^2} , \qquad (2)$$

where g is the gravity of Earth, h the satellite altitude and $\lambda = 2\pi c/\omega$ is the sent wavelength. For $\alpha = 0$, this phase-shift is of the order of few radians supposing $l = 6\,\mathrm{km}$, $\lambda = 800\,\mathrm{nm}$ and $h = 400\,\mathrm{km}$ [19].

However, the careful analysis of the optical COW in [21] showed that the first-order Doppler effect is roughly 10^5 times stronger than the desired signal φ_{gr}. This first-order Doppler effect was recently measured by exploiting large-distance precision interferometry along space channels [22], which represents a resource for performing fundamental tests of quantum mechanics in space, as in [18, 23–26], for future space-based scientific missions, such as LISA [27], and space-based quantum cryptography [28–32].

Here, we propose a novel test of the EEP exploiting a single EM-source and a double large-distance interferometric measurement performed at two different gravitational potentials. By comparing the phase-shifts obtained at a satellite and on Earth, it is possible to overcome the first-order Doppler effect affecting both the measurements and obtain the gravitational contribution. Such a scheme allows to bound the violation of LPI in the EM-sector with the precision on the order of 10^{-5}.

The proposal.—A possible setup for our proposal is sketched in Fig. 1 and is based on the satellite interferometry experiment realized in [22]. Such an interferometric measurement is obtained by sending a light pulse through a cascade of two fiber-based Mach Zehnder interferometers (MZIs) of equal temporal imbalance $\tau_l := nl/c$, with l denoting the length of the delay line and n the refraction coefficient of the fiber. In fact, after the first MZI the pulse is split into two temporal modes, called *short* ($\mathcal{S}$) and *long* ($\mathcal{L}$) depending on the path taken in the first MZI. The equal imbalance of the two MZIs guarantees that the two pulses are recombined (at the required level of precision) at the output of the second MZI, where they are detected. The combination of the possible paths the pulses may take leads to a characteristic detection pattern comprised of three possible arrival times for each pulse. The first (third) peak corresponds to the pulses that took the $\mathcal{S}$ ($\mathcal{L}$) path in both the MZIs, while the mid peak is due to the pulse that took the $\mathcal{S}$ path in the first interferometer and the $\mathcal{L}$ path in the subsequent one, or viceversa. Hence, interference is expected only in the central peak, due to the indistinguishability of the two possibilities.

Such interference is modulated by the phase difference φ accrued in the propagation, that depends on the relative motion between the ground station (GS) and the spacecraft (SC), as depicted in the bottom panel of Fig. 1, and on the difference in gravitational potentials, as we will detail in the following. From the ratio of the intensity of the central peak to the lateral ones an estimation of φ can be obtained [22]. For simplicity we assumed that the coherence time of the source τ_c is much shorter than the temporal imbalance τ_l ($\tau_c \ll \tau_l$), while the mismatch $\Delta \tau_l$ of the delay lines of the MZIs is $\Delta \tau_l < \tau_c$ (see Supplementary Material (SM), Sec. F for more details). Furthermore, we assumed that a single-mode coupling system is correctly implemented to guarantee the spatial overlap of the interfering beams and thus resulting in a high visibility. The latter assumption is demanding from the experimental point of view, requiring for example adaptive optics to correct wavefront distortion due to turbulence, but it is achievable with current technology [34, 35].

A bound on α will be retrieved from the difference of two phase-shifts φ_{SC} and φ_{GS}, each of which is obtained from a interferometric measurement of the kind described above. The first phase, φ_{SC}, is measured at detector A located on the SC while the second one, φ_{GS}, at detector B located at the GS by exploiting the reflection of the sent beam obtained with a corner-cube retroreflector (CCR) mounted on the satellite (Fig. 1).
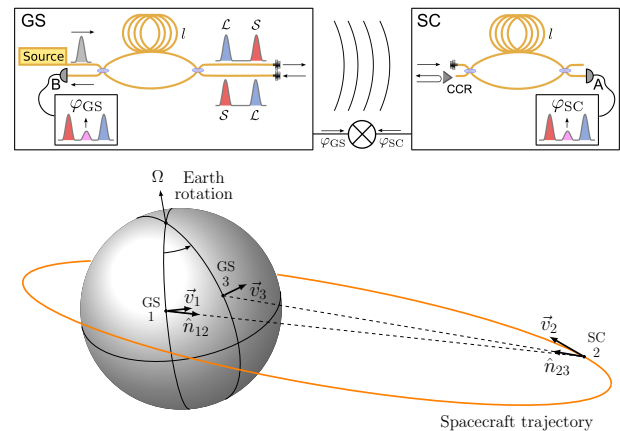

FIG. 1: (top) Scheme of the proposal. Both the GS and the SC are equipped with a MZI of equal delay line l. (bottom) Geometry of the experiment: $\vec{v}_1$ is the velocity of the GS at the emission at potential U_1; $\vec{v}_2$ is the velocity of the SC at the detection on the satellite at potential U_2; $\vec{v}_3$ is the velocity of the ground station at the detection of the beam retroreflected by the SC, which occurs at potential $U_3 = U_1$. Approximating Earth's angular velocity Ω as constant, $|\vec{v}_1|^2 = |\vec{v}_3|^2$. Vectors $\hat{n}_{12}$ and $\hat{n}_{23}$ are the Newtonian propagation directions of the light pulses.

Analysis of the proposal in the PPN approximation.—Now we present the detailed analysis of the phases to be measured by exploiting the the Parametrized Post Newtonian (PPN) formalism [3]. We use the notation of [21]. The spacetime metric has the signature $(-, +, +, +)$ and is denoted by $g_{\mu\nu}$. Since we deal with very short time intervals, we use an Earth-centered inertial system as the standard coordinate system. For brevity we refer to this coordinate system as "global", distinguishing it from the local frames that are established at the GS and the SC. Coordinates of events in these frames are distinguished by superscripts, such as t^{GS} and t^{SC}. The subscripts refer to the location of a particular event: 1 and 3 occur at the GS, event 2 at the SC (see Fig. 1). Frequencies ω_{ij} and unit vectors $\hat{n}_{ij}$ carry double subscripts indicating the locations of emission (i) and detection (j) events. Detailed relationships between the quantities, and relevant background about post-Newtonian propagation of light and interferometry are given in the SM, which provides a summary of the treatment of light propagation in the PPN formalism (Sec. A), phase calculation in gravitational field (Sec. B), and the detailed application to the setup we consider (Secs. C and D).

Our precision target is achieving a bound of $|\alpha| \lesssim \epsilon$ for light, with $\epsilon := \sqrt{U} \approx 10^{-5}$ where U is the approximate po-

tential for near-Earth experiments [2]: $U = GM_\oplus/(c^2 R_\oplus)$. The parameter ϵ sets the scaling order of PPN expansion around Earth. At this level of precision, we can ignore the effects of the gravitational field of other bodies in the Solar System, approximate the spacetime around the Earth as static, and consider only the leading (i.e. second order in ϵ) post-Newtonian effects [2, 21, 36]. Thus, the non-vanishing components of the metric in the PPN approximation are

$$g_{00} = -1 + 2U, \qquad g_{ij} = \delta_{ij}(1 + 2U). \qquad (3)$$

The most effective way to carefully estimate the accrued phases for the interfering beams in the scheme presented above is to use the geometry of Fig. 2, which represents the position of the GS and the SC at the different stages of the experiment. The interfering beams must take different paths in the passage through the two MZIs, one $\mathcal{S}$ path and one $\mathcal{L}$ path. Hence, at the satellite we will obtain interference between the beam that took the $\mathcal{L}$ path on Earth and the $\mathcal{S}$ one on the SC, that is

$$I_{A_1} := (\mathcal{L}^{\text{GS}}, \mathcal{S}^{\text{SC}}) : 1 \xrightarrow{l} 1^* \rightarrow 2^* , \qquad (4)$$

and the beam that passed the first time through the $\mathcal{S}$ path at the GS and then took the $\mathcal{L}$ one at the SC:

$$I_{A_2} := (\mathcal{S}^{\text{GS}}, \mathcal{L}^{\text{SC}}) : 1 \rightarrow 2 \xrightarrow{l} 2^* . \qquad (5)$$

In the above equations the numbers refer to the different events depicted in Fig. 2. Analogously, at the GS we will obtain interference between the beams

$$I_{B_1} := (\mathcal{L}^{\text{GS}}, \mathcal{S}^{\text{GS}}) : 1 \xrightarrow{l} 1^* \rightarrow 2^* \rightarrow 3^* , \qquad (6)$$

$$I_{B_2} := (\mathcal{S}^{\text{GS}}, \mathcal{L}^{\text{GS}}) : 1 \rightarrow 2 \rightarrow 3 \xrightarrow{l} 3^* , \qquad (7)$$

which are detected at the GS after being retroreflected by the CCR mounted on the SC.

The Doppler-cancellation scheme is based on the fact that the one-way GS→SC shifted frequencies, ω_{12} and $\omega_{1^*2^*}$, contain both the Doppler and gravitational contributions, while the two-way GS→SC→GS ones, ω_{13} and $\omega_{1^*3^*}$, are different from the initial frequency $\omega_{11} := \omega_0$ only due to the Doppler effect. This is because the gravitational contribution is cancelled out at the leading order in the two-way trip.

The signal from which a bound on α is obtained is a linear combination of the two measured phase-shifts

$$\varphi_{\text{SC}}(t_{2^*}^{\text{SC}}) := \Phi[I_{A_2}] - \Phi[I_{A_1}] , \qquad (8)$$

$$\varphi_{\text{GS}}(t_{3^*}^{\text{GS}}) := \Phi[I_{B_2}] - \Phi[I_{B_1}] , \qquad (9)$$

where $\Phi[I_X]$ denotes the phase accrued along the paths $I_X := (t_1, \vec{x}_1) \rightarrow (t, \vec{x})$ of Eqs. (4)-(7). $\Phi[I_X]$ is evaluated in the geometric optics approximation in the SM, which leads to

$$\Phi[I_X] = -\omega \left[(t - t_1) - \Delta t(\vec{x}; \vec{x}_1) \right] + \Phi_l , \qquad (10)$$

where the frequency $\omega = -k_0$ (denoting k^μ the wave 4-vector associated with the beam I_X) is constant along the
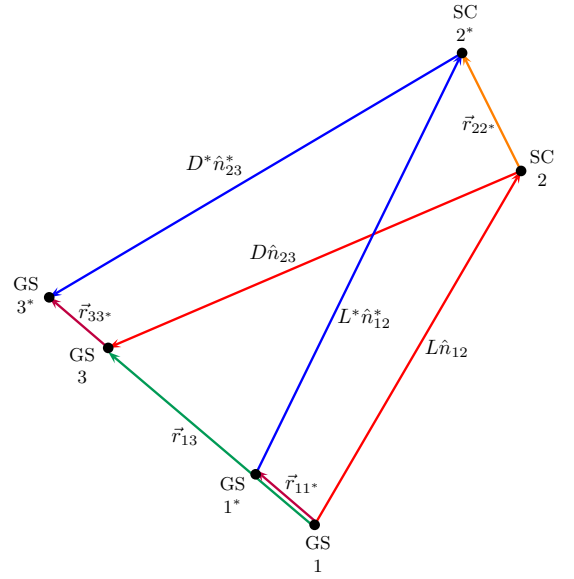

FIG. 2: Euclidean vectors representing positions of the GS and the SC at different stages of the experiment. Distances travelled by the beam on the go-return trip are L and D, respectively. At the leading (zeroth) order in ϵ, the round trip propagation time is $2T = 2L/c$, and the three vectors $\vec{r}_{11^*}$, $\vec{r}_{13}$ and $\vec{r}_{33^*}$ are parallel as depicted. Note that $|\vec{r}_{ij}| \ll L$. Mismatches in the arrival times of the pulses are discussed in SM, Sec. F.

null geodesic, $\Delta t(\vec{x}; \vec{x}_1)$ is the photon travel (coordinate) time along the geodesic, and Φ_l is the phase picked up passing through the delay line l, evaluated in the local reference frame.

With such an approach, the phase φ_{SC} evaluates to

$$\varphi_{\text{SC}}(t_{2^*}^{\text{SC}}) = (\omega_{12} - \omega_0)\tau_l - \omega_0\tau_l\mathfrak{s}_\uparrow + \delta\omega_0 t_{2^*}^{\text{SC}} , \qquad (11)$$

where τ_l is the proper time of the delay line, $\delta\omega_0 := \omega_{1^*2^*} - \omega_{12}$ is the leading term in the frequency difference at the satellite between the two beams I_{A_2} and I_{A_1} and $\omega_0\tau_l\mathfrak{s}_\uparrow := \omega_\uparrow^*\Delta t_{1^*2^*} - \omega_\uparrow\Delta t_{12}$ is the phase difference due to the difference in the coordinate propagation times Δt_{12} and $\Delta t_{1^*2^*}$ with $\omega_\uparrow$ and $\omega_\uparrow^*$ denoting the conserved frequencies in the global frame. All the quantities above are explicitly derived in the SM.

From Eq. (11) we see that three components contribute to φ_{SC}: the difference in phases accrued along the delay line, the phase difference between the different paths taken by the beams due to delay line, and a beat term due to a slight difference in frequencies as seen at the detector A, respectively.

Analogous considerations lead to the expression for the phase-shift φ_{GS} detected at the GS:

$$\varphi_{\text{GS}}(t_{3^*}^{\text{GS}}) = (\omega_{13} - \omega_0)\tau_l - \omega_0\tau_l(2\mathfrak{s}_\uparrow - 2\mathfrak{s}_\downarrow) + 2\delta\omega_0 t_{3^*}^{\text{GS}} , \qquad (12)$$

where $\omega_0\tau_l(\mathfrak{s}_\uparrow - 2\mathfrak{s}_\downarrow) := \omega_\downarrow^*\Delta t_{2^*3^*} - \omega_\downarrow\Delta t_{23}$ is the phase differences accrued during the downward propagation, which has to be added to the contribution $-\omega_0\tau_l\mathfrak{s}_\uparrow$ accrued during the upward propagation.

Both φ_{SC} and φ_{GS} contain terms of the first order in ϵ resulting from the first-order Doppler effect. Such terms are eliminated by manipulation of the corresponding data sets from the GS and SC in a manner similar to the time-delay interferometry techniques in Ref. [37]. The key feature allowing for this is that the ratio of the first order terms in φ_{SC} and φ_{GS} is exactly equal to two. Hence, adapting the techniques that were used for the data processing in the Gravity Probe A experiment [38], the signal

$$S := \varphi_{SC}(t_{2*}^{SC}) - \tfrac{1}{2}\varphi_{GS}(t_{3*}^{GS}) \qquad (13)$$

contains only second order terms and allows for the retrieval of the gravitational red-shift contribution $U_2 - U_1$. The explicit form of the signal is:

$$\frac{S}{\omega_0 \tau_l} = (1+\alpha)(U_2 - U_1) - \frac{2\left[\hat{n}_{12} \cdot (\vec{v}_1 - \vec{v}_2)\right]^2}{c^2}$$
$$+ \frac{3}{2}\frac{(\vec{v}_1 - \vec{v}_2)^2}{c^2} - \frac{[\vec{v}_2 \cdot (\vec{v}_2 - \vec{v}_1)]}{c^2} - \frac{2L\left[\hat{n}_{12} \cdot \vec{a}_1\right]}{c^2}, \quad (14)$$

where α parametrizes the violation of LPI, L is the zeroth order slant distance between the GS and the SC, $\vec{a}_1$ is the centripetal acceleration of the GS at 1, and the other vectors are specified in Fig. 1.

Simulations.—Now we present the numerical estimation of the signal derived above by exploiting the orbits of actual satellites used by the International Laser Ranging Service (ILRS) [39]. The Satellite Laser Ranging (SLR) technique allows for a high accuracy estimation of the distance of such satellites by measuring the time-of-flight of laser pulses that are sent from a GS on Earth, then retroreflected by the CCRs mounted on the orbiting terminal, and finally collected by the same GS. ILRS makes available the Consolidated Prediction Format [40] files for SLR orbits, which contain the geocentric (inertial Earth-centered) position of the terminals at a given time. Furthermore, ILRS offers a software routine [41] to estimate the motion of the ground-station in the same frame. Hence, we can simulate real passages of various SLR satellites as seen from an actual GS on Earth and then estimate the signals for such simulated orbits.

We specialized our simulations to two satellites in different orbits, Ajisai (circular orbit) and Galileo 201 (eccentric orbit). The used GS is the Matera Laser Ranging Observatory (MLRO) [42] of the Italian Space Agency, that was exploited for various demonstrations of the feasibility of satellite quantum communications [22, 23, 31, 43–45]. The upper panels of Fig. 3 show the signal $S/(\omega_0 \tau_l)$ from Eq. (14) as a function of the time passage for the two satellites, while the bottom panel are the signals estimated by supposing that such terminals are equipped with an unbalanced interferometer providing a delay line of $l = 100$ m ($\tau_l \approx 3 \cdot 10^{-7}$ s) and that the initial wavelength is $\lambda = 2\pi c/\omega_0 = 532$ nm. This choice of the parameters τ_l and ω_0 brings the strength of the signal in Eq. (14) into a measurable regime.

Conclusions.—Our proposal allows for the cancellation of the first-order Doppler effect in optical red-shift experiments.
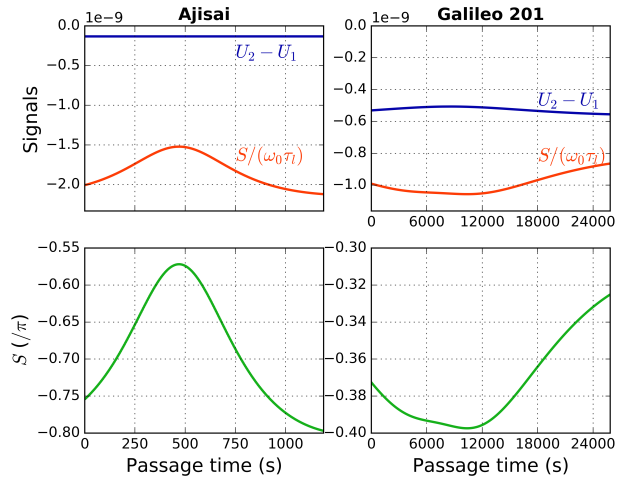

FIG. 3: Results obtained with Ajisai (left panels; inclination 50°, eccentricity 0.001, altitude 1,490 km) and Galileo 201 (right panels; inclination 50°, eccentricity 0.158, altitude ranging from 17,000 to 26,210 km) seen from the MLRO ground station. Upper panels show the signals $U_2 - U_1$ and $S/(\omega_0 \tau_l)$ from Eq. (14) (with $\alpha = 0$) as a function of the time passage. Bottom panels show the signal S (in π-unit) expected with a delay line $l = 100$ m and wavelength $\lambda = 532$ nm.

However, this proposal still faces two important practical issues. First, atmospheric turbulence is a limiting factor for large-distance optical interferometry. However, the planned temporal delay between the two pulses is four orders of magnitude lower than the conventional millisecond threshold of the turbulence correlation time [46]. As a result, both the interfering beams suffer through the same random noise that is canceled in measuring φ_{SC} and φ_{GS}. In fact, the same scale difference was successfully exploited in [22]. Second, the two delay lines cannot be perfectly identical. However, the relative precision $\delta_l \lesssim \epsilon$, which for $l = 100$ m translates into the absolute difference of less than 1 mm, is experimentally achievable. Its values can be retrieved by monitoring in real-time the first order interference at the two MZIs with a laser of long coherence time. In this case the signal $S/(\omega_0 \tau_l)$ gets a first-order constant offset δ_l, that can be reliably estimated and eliminated by using the SLR data. Moreover, the additional variable term of the order $\epsilon \delta_l$ can be eliminated similarly to the second order Doppler terms (see SM, Sec. F).

Concluding, in this work we proposed an optical scheme to bound the violation of the EEP in the electromagnetic sector of the Standard Model. In this scheme the first-order Doppler effect is suppressed and the weak gravitational red-shift can be measured. The need of new tests of physics and the recent advancements in satellite optical technologies make this proposal both attractive and feasible with current technologies. An in-depth investigation of the experimental design is a subject of forthcoming work.

———————

* Electronic address: daniel.terno@mq.edu.au
† Electronic address: paolo.villoresi@dei.unipd.it

[1] C. M. Will, *The Confrontation between General Relativity and Experiment*, Living Rev. Relativity **17**, 4 (2014)

[2] C. M. Will, *Theory and Experiment in Gravitational Physics*, (Cambridge University Press, 1993)

[3] E. Poisson and C. W. Will, *Gravity: Newtonian, Post-Newtonian, Relativistic*, (Cambridge University Press, 2014)

[4] P. A. M. Dirac, *The Cosmological Constants*, Nature **139**, 323 (1937)

[5] J.-P. Uzan, *Varying Constants, Gravitation and Cosmology*, Living Rev. Relativity **14**, 2 (2011)

[6] A. Einstein, Ann. Phys. **35**, 898 (1911)

[7] D. Colladay and V. A. Kostelecký, *Lorentz-violating extension of the standard model* , Phys. Rev. D **58**, 116002 (1998)

[8] V. A. Kostelecký and N. Russell, *Data tables for Lorentz and CPT violation*, Rev. Mod. Phys. **83**, 11 (2011)

[9] S. Liberatti, *Tests of Lorentz invariance: a 2013 update*, Class. Quantum Grav. **30**, 133001 (2013)

[10] M. A. Hohensee, S. Chu, A. Peters, and H. Müller, *Equivalence Principle and Gravitational Redshift*, Phys. Rev. Lett. **106**, 151102 (2011)

[11] J. Sakstein, *Tests of gravity with future space-based experiments*, Phys. Rev. D **97**, 064028 (2018)

[12] J. C. LoPresto, C. Schrader, and A. K. Pierce, *Solar gravitational redshift from the infrared oxygen triplet*, Astrophys. J **376**, 757 (1991)

[13] R. V. Pound and G. A. Rebka, Jr., *Apparent Weight of Photons*, Phys. Rev. Lett. **4**, 337 (1960)

[14] R. F. C. Vessot, M. W. Levine, E. M. Mattison, E. L. Blomberg, T. E. Hoffman, G. U. Nystrom, B. F. Farrel, R. Decher, P. B. Eby, C. R. Baugher, J. W. Watts, D. L. Teuber, and F. D. Wills, *Test of relativistic gravitation with a gpace-borne hydrogen maser*, Phys. Rev. Lett. **45**, 2081 (1980)

[15] F. Meynadier, P. Delva, C. le Poncin-Lafitte, C. Guerlin, and P. Wolf, *Atomic clock ensemble in space (ACES) data analysis*, Class. Quantum Grav. **35**, 035018 (2018)

[16] N. Ashby, T. E. Paker, and B. R. Patla, *A null test of general relativity based on a long-term comparison of atomic transition frequencies*, Nature Phys. **14**, 822-826 (2018)

[17] R. Colella, A. W. Overhauser, and S. Werner, *Observation of gravitationally induced quantum interference*, Phys. Rev. Lett. **34**, 1472 (1975)

[18] M. Zych, F. Costa, I. Pikovski, and Č. Brukner, *Quantum interferometric visibility as a witness of general relativistic proper time*, Nature Commun. **2**, 505 (2011)

[19] D. Rideout, T. Jennewein, G. Amelino-Camelia, T. F. Demarie, B. L. Higgins, A. Kempf, A. Kent, R. Laflamme, X. Ma, R. B. Mann, E. Martín-Martínez, N. C. Menicucci, J. Moffat, C. Simon, R. Sorkin, L. Smolin and D. R. Terno, *Fundamental quantum optics experiments conceivable with satellites-reaching relativistic distances and velocities*, Class. Quantum Grav. **29**, 224011 (2012)

[20] J. Brendel, N. Gisin, W. Tittel, H. Zbinden, *Pulsed Energy-Time Entangled Twin-Photon Source for Quantum Communication*, Phys. Rev. Lett. **82**, 2594 (1999)

[21] A. Broducth, A. Gilchrist, T. Guff, A R. H. Smith, D. R Terno, *Post-Newtonian gravitational effects in optical interferometry*, Phys. Rev. D **91**, 064041 (2015)

[22] G. Vallone, D. Dequal, M. Tomasin, F. Vedovato, M. Schiavon, V. Luceri, G. Bianco and P. Villoresi, *Interference at the single photon level along satellite-ground channels*, Phys. Rev. Lett. **116**, 253601 (2016)

[23] F. Vedovato, C. Agnesi, M. Schiavon, D. Dequal, L. Calderaro, M. Tomasin, D. G. Marangon, A. Stanco, V. Luceri, G. Bianco, G. Vallone and P. Villoresi, *Extending Wheeler's delayed-choice experiment to space*, Sci. Adv. **3**, e1701180 (2017)

[24] M. Zych, F. Costa, I. Pikovski, T. C. Ralph, and Č. Brukner, *General relativistic effects in quantum interference of photons*, Class. Quantum Grav. **29** 224010 (2012)

[25] J. Yin, Y. Cao, Y.-H. Li, S.-K. Liao, L. Zhang, J.-G. Ren, W.-Q. Cai, W.-Y. Liu, B. Li, H. Dai, G.-B. Li, Q.-M. Lu, Y.-H. Gong, Y. Xu, S.-L. Li, F.-Z. Li, Y.-Y. Yin, Z.-Q. Jiang, M. Li, J.-J. Jia, G. Ren, D. He, Y.-L. Zhou, X.-X. Zhang, N. Wang, X. Chang, Z.-C. Zhu, N.-L. Liu, Y.-A. Chen, C.-Y. Lu, R. Shu, C.-Z. Peng, J.-Y. Wang and J.-W. Pan, *Satellite-based-entanglement distribution over 1200 kilometers*, Science **356** (6343), 1140-1144 (2017)

[26] J.-G. Ren, P. Xu, H.-L. Yong, L. Zhang, S.-K. Liao, J. Yin, W.-Y. Liu, W.-Q. Cai, M. Yang, L. Li, K.-X. Yang, X. Han, Y.-Q. Yao, J. Li, H.-Y. Wu, S. Wan, L. Liu, D.-Q. Liu, Y.-W. Kuang, Z.-P. He, P. Shang, C. Guo, R.-H. Zheng, K. Tian, Z.-C. Zhu, N.-L. Liu, C.-Y. Lu, R. Shu, Y.-A. Chen, C.-Z. Peng, J.-Y. Wang and J.-W. Pan, *Ground-to-satellite quantum teleportation*, Nature **549**, 70-73 (2017)

[27] K. Danzmann and the LISA study team, *LISA: laser interferometer space antenna for gravitational wave measurements*, Class. Quantum Grav. **13**, A247 (1996)

[28] S.-K. Liao, W.-Q. Cai, W.-Y. Liu, L. Zhang, Y. Li, J.-G. Ren, J. Yin, Q. Shen, Y. Cao, Z.-P. Li, F.-Z. Li, X.-W. Chen, L.-H. Sun, J.-J. Jia, J.-C. Wu, X.-J. Jiang, J.-F. Wang, Y.-M. Huang, Q. Wang, Y.-L. Zhou, L. Deng, T. Xi, L. Ma, T. Hu, Q. Zhang, Y.-A. Chen, N.-L. Liu, X.-B. Wang, Z.-C. Zhu, C.-Y. Lu, R. Shu, C.-Z. Peng, J.-Y. Wang and J.-W. Pan, *Satellite-to-ground quantum key distribution*, Nature **549**, 43-47 (2017)

[29] D. K. L. Oi, A. Ling, G. Vallone, P. Villoresi, S. Greenland, E. Kerr, M. Macdonald, H. Weinfurter, H. Kuiper, E. Charbon and R. Ursin, *CubeSat quantum communications mission*, EPJ Quantum Technology **4**, 6 (2017)

[30] R. Bedington, J. M. Arrazola and A. Ling, *Progress in satellite quantum key distribution*, npj Quantum Information **3**, 30 (2017)

[31] C. Agnesi, F. Vedovato, M. Schiavon, D. Dequal, L. Calderaro, M. Tomasin, D. G. Marangon, A. Stanco, V. Luceri, G. Bianco, G. Vallone, P. Villoresi, *Exploring the boundaries of quantum mechanics: advances in satellite quantum communications*, Phil. Trans. R. Soc. A **376**, 20170461 (2018)

[32] I. Khan, B. Heim, A. Neuzner, C. Marquardt, *Satellite-Based QKD*, Optics and Photonics News **29**, (2018)

[33] S.-K. Liao, W.-Q. Cai, J. Handsteiner, B. Liu, J. Yin, L. Zhang, D. Rauch, M. Fink, J.-G. Ren, W.-Y. Liu, Y. Li, Q. Shen, Y. Cao, F.-Z. Li, J.-F. Wang, Y.-M. Huang, L. Deng, T. Xi, L. Ma, T. Hu, L. Li, N.-L. Liu, F. Koidl, P. Wang, Y.-A. Chen, X.-B. Wang, M. Steindorfer, G. Kirchner, C.-Y. Lu, R. Shu, R. Ursin, T. Scheidl, C.-Z. Peng, J.-Y. Wang, A. Zeilinger and J.-W. Pan, *Satellite-Relayed Intercontinental Quantum Network*, Phys. Rev. Lett **120**, 030501 (2018)

[34] H. Takenaka, M. Toyoshima, and Y. Takayama, *Experimental*

verification of fiber-coupling efficiency for satellite-to-ground atmospheric laser downlinks, Opt. Express **20**, 15301 (2012)

[35] M. W. Wright, J. F. Morris, J. M. Kovalik, K. S. Andrews, M. J. Abrahamson, and A. Biswas, *Adaptive optics correction into single mode fiber for a low Earth orbiting space to ground optical communication link using the OPALS downlink*, Opt. Express **23**, 33705(2015)

[36] I. Ciufolini and J. A. Wheeler, *Gravitation and inertia*, (Princeton University Press, 1995)

[37] M. Tinto and S. V. Dhurandhar, *Time-Delay Interferometry*, Living Rev. Relativity **17**, 6 (2014)

[38] R. F. C. Vessot and M. W. Levine, *Gravitational redshift space-probe experiment*, NASA technical report NASA-CR-161409, 1979)

[39] M.R. Pearlman, J.J Degnan, and J.M. Bosworth, *The International Laser Ranging Service*, Advances in Space Research **30**, 135-143 (2002)

[40] https://ilrs.cddis.eosdis.nasa.gov/data_and_products/formats/cpf.html

[41] https://ilrs.cddis.eosdis.nasa.gov/technology/software/index.html

[42] https://ilrs.cddis.eosdis.nasa.gov/network/stations/active/MATM_general.html

[43] G. Vallone, D. Bacco, D. Dequal, S. Gaiarin, V. Luceri, G. Bianco and P. Villoresi, *Experimental satellite quantum communications*, Phys. Rev. Lett. **115**, 040502 (2015)

[44] D. Dequal, G. Vallone, D. Bacco, S. Gaiarin, V. Luceri, G. Bianco and P. Villoresi, *Experimental single-photon exchange along a space link of 7000 km*, Phys. Rev. A **93**, 010301(R) (2016)

[45] L. Calderaro, C. Agnesi, D. Dequal, F. Vedovato, M. Schiavon, A. Santamato, V. Luceri, G. Bianco, G. Vallone and P. Villoresi, *Towards Quantum Communication from Global Navigation Satellite System*, arXiv:1804.05022 [quant-ph]

[46] J. W. Goodman, *Statistical Optics*, 2nd edition (John Wiley, Hoboken, 2015)

SUPPLEMENTARY MATERIAL

Discussion of light propagation and locally observed frequencies at the leading order of the post-Newtonian approximation is given in Sec. A. Accumulation of interferometric phase in the relativistic framework is discussed in Sec. B. We describe the details of the path difference and frequencies calculations in Sec. C, and provide the expressions for phase differences at the two detection events, as well as analyze the the mismatch in the arrival times in Sec. D. The final expression for the signal is obtained in Sec. E, and the effects of unequal imbalance between the interferometers are treated in Sec. F.

For simplicity we set $c = 1$ in Secs. A and B. Further, coordinates of an event are labeled by $x^\mu = (t, \vec{x})$, where $\vec{x}$ stands for three spacelike coordinates in any spacetime. A vector in a three-dimensional Euclidian space is denoted as $\vec{a}$, and is equipped with the usual Euclidian inner product $\vec{x} \cdot \vec{y} = x^1 y^1 + x^2 y^2 + x^3 y^3$. Hence, $\hat{n} = \vec{n}/\vec{n} \cdot \vec{n}$ is a unit Euclidean vector, and the coordinate distance is $r := \sqrt{\vec{x} \cdot \vec{x}}$. 4-vectors are denoted in arial font, u, and their components with Greek superscripts, u^μ. To simplify the formulas we write expression like ω_{1*2*} as ω_{12}^*.

A. Light propagation in the leading order PPN formalism

A detailed exposition of the PPN formalism and its application to light can be found in [2, 3]. The metric with including the leading post-Newtonian terms (up to the second order in ϵ) is given by

$$g_{00} = -1 + 2U, \qquad g_{ij} = \delta_{ij}(1 + 2U), \tag{S-1}$$

with $U = \frac{GM}{r} Q(r, \theta)$ denoting the gravitational potential around the Earth including the quadrupole term [36]

$$Q(r, \theta) := 1 - \tfrac{1}{2} J_2 \frac{R^2}{r^2} (3 \cos^2 \theta - 1), \tag{S-2}$$

where $J_2 = 1.083 \times 10^{-3}$ is the normalized quadrupole moment and the higher terms are neglected. R is the Earth equatorial radius. Given the established bounds on the PPN parameter γ [1] we set $(1 + \gamma) = 2$ in the PPN metric of Eq. (3).

The 4-velocity of a massive particle is

$$\mathsf{u} = \frac{dt}{d\tau}(1, \vec{v}) =: \upsilon(1, \vec{v}), \qquad \mathsf{u}^2 = -1, \tag{S-3}$$

where τ is the proper time and for a given $\vec{v}$ the constant υ is obtained from the normalization with the post-Newtonian metric of Eq. (3), The wave 4-vector is given by

$$\mathsf{k} = \frac{dt}{d\sigma}\left(1, \frac{d\vec{r}}{dt}\right) =: \kappa(1, \vec{k}), \qquad \mathsf{k}^2 = 0, \tag{S-4}$$

where σ is an affine parameter and we have defined the parameter κ, which is determined by the frequency measured by a stationary observer in the given reference frame. The vector $\vec{k}$ may be expanded in the PPN parameter ϵ as

$$\vec{k} = \hat{n} + \epsilon^2 \vec{k}_{(2)} + \epsilon^3 \vec{k}_{(3)} + \dots, \tag{S-5}$$

where $\hat{n}$ is a unit Euclidean vector giving the Newtonian light propagation. Here and in the expansions below we occasionally use ϵ as a formal parameter that tracks the orders of perturbation and is set to 1 in final expressions. For the frequency and phase calculations at the second order of ϵ it is enough to work with $\vec{k} = \hat{n}$.

In a stationary metric the quantity k_0 is conserved. Therefore the conserved frequency at any point along the trajectory of the light beam, up to the second order in ϵ, is

$$\omega = -k_0 = \kappa(1 - 2\epsilon^2 U). \tag{S-6}$$

The frequency as seen in the proper frame of an observer that moves with the 4-velocity $\mathsf{u} = \upsilon_{\mathsf{u}}(1, \vec{v})$ is

$$\omega^{(\mathsf{u})} = -\mathsf{k} \cdot \mathsf{u} = \kappa \upsilon_{\mathsf{u}}(1 - \epsilon \hat{n} \cdot \vec{v} - \epsilon^2 2U), \tag{S-7}$$

where U is evaluated at the location of the observer.

With introduction of

$$q := -\mathsf{k} \cdot \mathsf{u}/\kappa \upsilon_{\mathsf{u}}, \tag{S-8}$$

a local frequency in any frame can be written as a product of three factors, $\omega^{(\mathsf{u})} = \kappa v_{\mathsf{u}} q$. This decomposition conveniently separates different parts of the four-vectors. For example, if the signal was sent from the location i then at j the local frequency is determined by

$$q_{ij} = -\mathsf{k}_i(t_j) \cdot \mathsf{u}_j / \kappa_{ij} v_j \tag{S-9}$$

and has a value ω_{ij}.

B. Interferometry: phase calculations, moving frames, and curved space

We now describe light wave propagation and the acquired phase using geometric optics. The scalar wave amplitude of a beam of light is $A(x)e^{i\Phi(x)}$, where the phase Φ satisfies the eikonal equation, which amounts to the Hamilton-Jacobi equation for massless particles. As a consequence we will refer to fictitious photons traveling along the trajectories of the light beams. We speak conventionally about the interference or detection at the spacetime point $x = (t, \vec{x})$, while the origin of the beam(s) is at $x_1 = (t_1, \vec{x}_1)$, etc.

In a stationary spacetime for a beam approximated by a geodesic segment between x_1 and x, the acquired phase is given by

$$\Phi(x) = -\omega[(t - t_1) - S(\vec{x}; \vec{x}_1)] + \tilde{\Phi}_1 := -\omega\big(t - S(\vec{x}; \vec{x}_1)\big) + \Phi_1, \tag{S-10}$$

where the "abbreviated action" S satisfies $S(\vec{x}_1; \vec{x}_1) = 0$. On a curved stationary background (the timelike Killing vector is tangent to the time coordinate t) the frequency ω is a conserved quantity $-k_0$, and t is the coordinate time.

On each trajectory of a fictitious massless point particle (photon) the phase is constant. Light rays guide the propagation of surfaces of constant phase, and the function $S(\vec{x}, \vec{x}_1)$ can be expressed via the photon travel time along the geodesic as

$$S(\vec{x}; \vec{x}_1) = \Delta t(\vec{x}; \vec{x}_1), \tag{S-11}$$

i.e.

$$\Phi(x) = -\omega\big(t - \Delta t(\vec{x}; \vec{x}_1)\big) + \Phi_1. \tag{S-12}$$

Introducing a local orthonormal basis e_a, $a = 0, \ldots 3$, so any vector is expressed as $\mathsf{k} = k^a \mathsf{e}_a$, we can (locally) write the phase as

$$\Phi(x) = k^a x_a + \Psi_1 = k^\mu x_\mu + \Psi_1, \tag{S-13}$$

where the last expression holds if the origin of the coordinate frame $(\partial/\partial t, \partial/\partial \vec{x})$ coincides with the origin of the orthonormal frame. If it is possible (e.g. for a single beam) to choose a frame where the coordinates are adjusted to $x = 0$, then

$$\Psi_1 = \Phi_1 + \Delta t(\vec{x} = 0; \vec{x}_1)\omega. \tag{S-14}$$

The frequency that is measured by an observer at rest in this frame is $\omega_{\mathcal{S}} = -k_{a=0}$. In a different Lorentz frame $\mathcal{S}'$ [that has the same origin and is related by an arbitrary combination of boosts and rotations to the original orthonormal frame] the phase is expressed as

$$\Phi(x') = k'^a x'_a + \Psi_1, \tag{S-15}$$

with the same accrued phase Ψ_1.

If a pulse is reflected off a moving mirror, then by observing that

$$\Phi(x_2) = -\omega t_2 + \Phi_1 + \omega \Delta t(\vec{x}_2; \vec{x}_1) =: -\omega t_2 + \Phi_2, \tag{S-16}$$

and writing the reflected wave four-vector as $\tilde{\mathsf{k}}$ (in general $\omega \neq \tilde{\omega}$), we have for $t > t_2$

$$\Phi(x) = -\tilde{\omega}\big(t - \Delta t(\vec{x}; \vec{x}_2)\big) + \Phi_1 + \omega \Delta t(\vec{x}_2; \vec{x}_1) = -\tilde{\omega}\big(t - \Delta t(\vec{x}; \vec{x}_2)\big) + \Phi_2. \tag{S-17}$$

C. Frequencies and path differences

C.1 Relationship between trajectory parameters

We give a detailed derivation of the relationship between $\hat{n}_{12}$ and $\hat{n}_{23}$. Elementary geometry based on Fig. 2 gives

$$\vec{r}_{13} =: \hat{n}_{12}L + \hat{n}_{23}D. \tag{S-18}$$

Let us define the vector $\vec{\nu}$ as

$$\hat{n}_{23} =: -\hat{n}_{12} + \epsilon\vec{\nu}, \quad \hat{n}_{12} \cdot \vec{\nu} = 0, \tag{S-19}$$

and the quantity Λ as

$$D =: L(1 + \epsilon\Lambda). \tag{S-20}$$

At zeroth order in ϵ, the time taken for the return trip of beam $I_{1\to2\to3}$ is $(L + D)/c = 2L/c = 2T$, so Eq. (S-18) becomes (we set $\vec{\beta}_i := \vec{v}_i/c$ and $\mathfrak{d}_i = \hat{n}_{12} \cdot \vec{\beta}_i$)

$$2\vec{\beta}_1 = -\hat{n}_{12}\Lambda + \vec{\nu}, \tag{S-21}$$

resulting in the first order corrections

$$D = L(1 - 2\hat{n}_{12} \cdot \vec{\beta}_1), \qquad \hat{n}_{23} = -\hat{n}_{12}(1 + 2\hat{n}_{12} \cdot \vec{\beta}_1) + 2\vec{\beta}_1, \tag{S-22}$$

that is,

$$\Lambda = -2\mathfrak{d}_1, \qquad \vec{\nu} = -2\hat{n}_{12}\mathfrak{d}_1 + 2\vec{\beta}_1. \tag{S-23}$$

Other relationships are obtained similarly. Parameters of the 1^*2^* segment are given as

$$\hat{n}_{12}^* =: \hat{n}_{12} + \mu\vec{\nu}_{12}, \quad \hat{n}_{12} \cdot \vec{\nu}_{12} = 0, \tag{S-24}$$

where the above equations define the vector

$$\vec{\nu}_{12} = n(\vec{\beta}_2 - \vec{\beta}_1) - n\hat{n}_{12}(\mathfrak{d}_2 - \mathfrak{d}_1) \tag{S-25}$$

and $\mu := l/L$, and

$$L^* = L(1 + \mu\ell). \tag{S-26}$$

To leading order in μ they are

$$(L^* - L) = \tau_l\hat{n}_{12} \cdot (\vec{v}_2 - \vec{v}_1) = L \cdot \mathcal{O}(\mu\epsilon), \qquad |\hat{n}_{12} - \hat{n}_{12}^*| = \mathcal{O}(\mu\epsilon). \tag{S-27}$$

The term of the order of μ^2 carries with it a factor of the order ϵ^2, and therefore this term is small enough to be ignored at our level of approximation and is undefined without taking into account the post-Newtonian correction to the orbit.

To find the relationship between the segments 23 and 2^*3^* we note that the difference between $\vec{\beta}_1$ and $\vec{\beta}_3$ is of the order of ϵ^2. Indeed, the centripetal acceleration at the Earth's surface is $a = v_E^2/R\cos\vartheta$, where $\vartheta = \pi/2 - \theta_E$ denotes the latitude of the ground station. The Earth's acceleration is of the order v_E^2/R so we may use its values at either points 1 or 3. Hence for

$$\hat{n}_{23}^* = \hat{n}_{23} + \mu\vec{\nu}_{23}, \quad \hat{n}_{23} \cdot \vec{\nu}_{23} = 0, \qquad D^* = D(1 + \mu d) = L^*(1 + \epsilon\Lambda^*), \tag{S-28}$$

and

$$D^* =: L(1 + \epsilon\Lambda + \mu d) := L(1 + \mu\ell + \epsilon\Lambda^*). \tag{S-29}$$

we obtain

$$d = n\hat{n}_{23} \cdot (\vec{\beta}_1 - \vec{\beta}_2) = n(\mathfrak{d}_2 - \mathfrak{d}_1) = \ell, \tag{S-30}$$

and

$$\vec{\nu}_{23} = -n(\vec{\beta}_2 - \vec{\beta}_1) - n\hat{n}_{23}[\hat{n}_{23} \cdot (\vec{\beta}_1 - \vec{\beta}_2)] = -n(\vec{\beta}_2 - \vec{\beta}_1) + n\hat{n}_{12}(\mathfrak{d}_2 - \mathfrak{d}_1) = -\vec{\nu}_{12} \tag{S-31}$$

C.2 Frequencies

The standard second-order expression for the frequencies detected at the satellite

$$\frac{\omega_{12}}{\omega_0} = \left(\frac{1 - U_1 - \frac{1}{2}\beta_1^2}{1 - U_2 - \frac{1}{2}\beta_2^2}\right)\left(\frac{1 - \hat{n}_{12}\cdot\vec{\beta}_2}{1 - \hat{n}_{12}\cdot\vec{\beta}_1}\right), \tag{S-32}$$

and at the ground station after a go-return trip,

$$\frac{\omega_{13}}{\omega_0} = \left(\frac{1 - \hat{n}_{23}\cdot\vec{\beta}_3}{1 - \hat{n}_{23}\cdot\vec{\beta}_2}\right)\left(\frac{1 - \hat{n}_{12}\cdot\vec{\beta}_2}{1 - \hat{n}_{12}\cdot\vec{\beta}_1}\right). \tag{S-33}$$

Assuming the light source is stable, the proper frequencies of the beam at GS is not changing. However,

$$\frac{\omega_{12}^*}{\omega_0} = \left(\frac{1 - U_1 - \frac{1}{2}\beta_1^2}{1 - U_2^* - \frac{1}{2}\beta_2^{*2}}\right)\left(\frac{1 - \hat{n}_{12}^*\cdot\vec{\beta}_2^*}{1 - \hat{n}_{12}^*\cdot\vec{\beta}_1^*}\right). \tag{S-34}$$

The leading term in the difference $\omega_{12}^* - \omega_{12}$ comes from the terms of the order ϵ and is itself of the order $\mu\epsilon^2$

$$\delta_1 := \frac{\omega_{12}^* - \omega_{12}}{\omega_0} = \hat{n}_{12}\cdot(\vec{\beta}_2 - \vec{\beta}_1) - \hat{n}_{12}^*\cdot(\vec{\beta}_2^* - \vec{\beta}_1^*) = -\mu\vec{\nu}_{12}\cdot(\vec{\beta}_2 - \vec{\beta}_1) - \hat{n}_{12}\cdot(\vec{g}_2 - \vec{a}_1)\tau_l/c. \tag{S-35}$$

Using the value of $\vec{\nu}_{12}$ from Eq. (S-25) we obtain

$$\delta_1 = -n\mu\big[(\vec{\beta}_2 - \vec{\beta}_1)^2 - (\mathfrak{d}_2 - \mathfrak{d}_1)^2\big] - \hat{n}_{12}\cdot(\vec{g}_2 - \vec{a}_1)\tau_l/c. \tag{S-36}$$

Next, we assume that the experiment is performed during the ballistic part of the trajectory, so $\vec{a}_2 = \vec{g}_2$, where $g_2/c^2 \sim U_2/L$ is the free fall acceleration. Since $a \sim v^2/L$ the relative difference in frequencies is of the order $\mu\epsilon^2 \sim \epsilon^2\tau_l/L$. For $\omega_0 \sim$ 500 THz and $\mu \sim 10^{-4} - 10^{-5}$ it gives the beat frequency at the order of $1 - 30$Hz.

The frequency of the beam arriving at GS at 3^* from the satellite at 2^* is

$$\frac{\omega_{13}^*}{\omega_0} = \left(\frac{1 - \hat{n}_{23}^*\cdot\vec{\beta}_3^*}{1 - \hat{n}_{23}^*\cdot\vec{\beta}_2^*}\right)\left(\frac{1 - \hat{n}_{12}^*\cdot\vec{\beta}_2^*}{1 - \hat{n}_{12}^*\cdot\vec{\beta}_1^*}\right) \tag{S-37}$$

resulting in the difference

$$\frac{\omega_{13}^* - \omega_{13}}{\omega_0} = \hat{n}_{12}\cdot(\vec{\beta}_2 - \vec{\beta}_1) - \hat{n}_{12}^*\cdot(\vec{\beta}_2^* - \vec{\beta}_1^*) + \hat{n}_{23}\cdot(\vec{\beta}_3 - \vec{\beta}_2) - \hat{n}_{23}^*\cdot(\vec{\beta}_3^* - \vec{\beta}_2^*) = \delta_1 + \delta_2, \tag{S-38}$$

where

$$\delta_2 := \hat{n}_{23}\cdot(\vec{\beta}_3 - \vec{\beta}_2) - \hat{n}_{23}^*\cdot(\vec{\beta}_3^* - \vec{\beta}_2^*) = \mu\vec{\nu}_{12}\cdot(\vec{\beta}_3 - \vec{\beta}_2) - \hat{n}_{23}\cdot(\vec{a}_3 - \vec{g}_2)\tau_l/c. \tag{S-39}$$

Since the difference between $\vec{v}_3$ and $\vec{v}_1$ is of the order of ϵ^2, $\vec{v}_1$ and $\vec{a}_1$ can be used in the above formula. Therefore

$$\delta_2 = \mu\vec{\nu}_{12}\cdot(\vec{\beta}_1 - \vec{\beta}_2) + \hat{n}_{12}\cdot(\vec{a}_1 - \vec{g}_2)\tau_l/c = -\big[(\vec{\beta}_2 - \vec{\beta}_1)^2 - (\mathfrak{d}_2 - \mathfrak{d}_1)^2\big]\tau_l/T - \hat{n}_{12}\cdot(\vec{g}_2 - \vec{a}_1)\tau_l/c = \delta_1 \tag{S-40}$$

where $T := L/c$. Given Eq. (S-40), we set $\delta := \delta_1 = \delta_2$ for what follows.

The upward propagating beams are described by the wave vectors

$$\mathsf{k}_1(t_1) = \kappa_{11}\big(1, \hat{n}_{12}\big), \qquad \mathsf{k}_1^*(t_1^*) = \kappa_{11}^*\big(1, \hat{n}_{12}^*\big), \tag{S-41}$$

and so the conserved frequencies are $\omega_\uparrow := (\mathsf{k}_1)_0 = \kappa_{11}(1 - 2U_1)$ and $\omega_\uparrow^* = \kappa_{11}^*(1 - 2U_1)$, respectively. Similarly, the two conserved frequencies of the downward propagation are $\omega_\downarrow = \kappa_{22}(1 - 2U_2)$ and $\omega_\downarrow^* = \kappa_{22}^*(1 - 2U_2)$ (the difference between U_2 and U_2^* is of the order $\mu\epsilon^3$). These frequencies are

$$\frac{\omega_\uparrow}{\omega_0} = 1 + \mathfrak{d}_1 + \big(-U_1 + \mathfrak{d}_1^2 - \tfrac{1}{2}\beta_1^2\big), \tag{S-42}$$

and

$$\omega_\uparrow^* = \omega_\uparrow + \omega_0(\mu\vec{v}_{12} \cdot \vec{\beta}_1 + \hat{n}_{12} \cdot \vec{a}_1\tau_l/c). \tag{S-43}$$

Equations (S-42) and (S-43) imply

$$\omega_\uparrow^* - \omega_\uparrow = \omega_0\tau_l \left(\frac{\vec{\beta}_1 \cdot (\vec{\beta}_2 - \vec{\beta}_1) - \mathfrak{d}_1(\mathfrak{d}_2 - \mathfrak{d}_1)}{T} + \frac{\hat{n}_{12} \cdot \vec{a}_1}{c} \right). \tag{S-44}$$

Upon reflection $\kappa_{22} = \omega_{12}/(q_{22}v_2)$. Accordingly,

$$\frac{\omega_\downarrow}{\omega_0} = \frac{\kappa_{11}}{\omega_0} - 2\vec{\beta}_2 \cdot \hat{n}_{12} - 2U_1 + 2(\hat{n}_{12} \cdot \vec{\beta}_2)^2 - 2(\hat{n}_{12} \cdot \vec{\beta}_1)(\vec{\beta}_2 \cdot \hat{n}_{12}) + \vec{\beta}_2 \cdot \vec{\nu}, \tag{S-45}$$

and

$$\omega_\downarrow^* = \omega_\uparrow^* - 2\omega_0(\mu\vec{\beta}_2 \cdot \vec{v}_{12} + \hat{n}_{12} \cdot \vec{a}_2\tau_l/c). \tag{S-46}$$

C.3 Propagation times

At zeroth order in ϵ the upward and downward propagation times coincide, $T = L/c$. The second order expressions (that include the Shapiro time delay) are

$$\Delta t_{12} =: T + \tau_{\text{up}}, \qquad \Delta t_{23} =: D/c + \tau_{\text{down}} \tag{S-47}$$

for the upward and downward propagation, respectively. Here we used the approximation $Q = 1$ (uniform spherical Earth), which does not cause a loss in precision as the $\tau_{\text{up/down}}$ corrections cancel out below and their explicit form is not necessary. Indeed,

$$\Delta t_{12}^* = \frac{L^*}{c} + \tau_{\text{up}}, \qquad \Delta t_{23}^* = \frac{D^*}{c} + \tau_{\text{down}}, \tag{S-48}$$

where the dropped terms are of the order of $\mu\epsilon^3$.

D. Phases differences

Even under the ideal conditions the two pulses that are separated at the moment t_1 and follow the delay line and the free space travel in different order will arrive to the detectors A and B at slightly different times. The mismatch that we evaluate below should be much smaller then the coherence time of the pulses.

The pulses I_{A_1} (blue line on Fig. 2, the delay loop on the ground is followed by the upward path to the satellite) and I_{B_2} (red line on Fig. 2, the upward path to the satellite is followed by the delay there), that were produced at t_1 arrive to the detector A at t_{2^*} and t_{II}, respectively. They accrue the phases

$$\Psi_1^A = \omega_{11}\tau_l + \omega_\uparrow^*\Delta t_{12}^*, \qquad \Psi_2^A = \omega_\uparrow\Delta t_{12} + \omega_{12}\tau_l, \tag{S-49}$$

and hence at the respective moments of arrival the signal is given by

$$\Phi[I_{A_1}] = -\omega_{12}^* t_{2^*}^{\text{SC}} + \Psi_1^A, \qquad \Phi[I_{A_2}] = -\omega_{12} t_{\text{II}}^{\text{SC}} + \Psi_2^A, \tag{S-50}$$

respectively.

At leading order in ϵ the mismatch between the arrival of pulses I_{A_1} (at $t_{2^*}^{\text{SC}}$) to the satellite and completion of the loop by beam I_{A_2} onboard (at $t_{\text{II}}^{\text{SC}}$) is due to the difference in their travel times,

$$\Delta T := t_{2^*}^{\text{SC}} - t_{\text{II}}^{\text{SC}} = \frac{L^* - L}{c} = \tau_l(\mathfrak{d}_2 - \mathfrak{d}_1). \tag{S-51}$$

This means that at the point $\vec{x}_{2^*}$, the beam that left the ground station at $t_{1^*}^{\text{GS}}$ meets not the beam from which it was split at $t_1^{\text{GS}} := t_{1^*}^{\text{GS}} - \tau_l$, but the beam that left the ground station at $t_{1-}^{\text{GS}} := t_1^{\text{GS}} + \Delta T$. (The time intervals that correspond to the same

spatial location differ between the three frames we use by the expression of the order of ϵ^2, while due to the changes in the state of the motion the correction terms themselves differ by the terms of the order ϵ^3 or higher).

Hence the correct beat term at the time t_{2*}^{SC} is then

$$\varphi_{\text{SC}}^{\text{beats}}(t_{2*}^{\text{SC}}) = (\omega_{1*2*} - \omega_{1-2*})t_{2*}^{\text{SC}}, \tag{S-52}$$

However, using Eq. (S-35) we see that indicates that the corrected frequency difference is

$$\omega_{1*2*} - \omega_{1-2*} = \omega_{1*2*} - \omega_{12} - (\omega_{1-2*} - \omega_{12}) = \delta\omega_0\big(1 + \mathcal{O}(\epsilon)\big). \tag{S-53}$$

Since we are interested in the phase differences up to the second order in ϵ and the correction due to the time difference is of the order $\mathcal{O}(\delta\epsilon) = \mathcal{O}(\epsilon^3)$ we can approximate the phase-shift $\varphi_{\text{SC}}(t_{2*}^{\text{SC}})$ as

$$\varphi_{\text{SC}}(t_{2*}^{\text{SC}}) = \Phi[I_{A_2}] - \Phi[I_{A_1}] = (\omega_{12}^* - \omega_{12})t_{2*}^{\text{SC}} + (\omega_{12} - \omega_{11})\tau_l + \omega_\uparrow\Delta t_{12} - \omega_\uparrow^*\Delta t_{12}^*, \tag{S-54}$$

obtaining Eq. (11).

Similarly, at the detector B, where the pulses I_{B_1} (blue line on Fig. 2) and I_{B_2} (red line on on Fig. 2) that were produced at t_1 arrive at the moments t_{III} and t_{3*}, respectively. Their phases at B are

$$\Phi[I_{B_1}] = -\omega_{13}^* t_{3*}^{\text{GS}} + \omega_{11}\tau_l + \omega_\uparrow^*\Delta t_{12}^* + \omega_\downarrow^*\Delta t_{23}^*, \qquad \Phi[I_{B_2}] = -\omega_{13}t_{\text{III}}^{\text{GS}} + \omega_\uparrow\Delta t_{12} + \omega_\downarrow\Delta t_{23} + \omega_{13}\tau_l, \tag{S-55}$$

respectively. Hence with the relative precision ϵ the difference in the arrival times,

$$t_{3*}^{\text{GS}} - t_{\text{III}}^{\text{GS}} = \frac{D^* - D}{c} + \frac{L^* - L}{c} = 2\tau_l(\mathfrak{d}_2 - \mathfrak{d}_1). \tag{S-56}$$

Similarly, the signal $\varphi_{\text{GS}}(t_{3*}^{\text{GS}})$ results from the phase difference between beam I_{B_2} (loop on the ground, go-return trip to the satellite) and beam I_{B_1} (go-return trip to the satellite, loop on the ground). The phase acquired by the beams along both paths are

$$\Psi_1^B = \omega_{11}\tau_l + \omega_\uparrow^*\Delta t_{12}^* + \omega_\downarrow^*\Delta t_{23}^*, \qquad \Psi_2^B = \omega_\uparrow\Delta t_{12} + \omega_\downarrow\Delta t_{23} + \omega_{13}\tau_l. \tag{S-57}$$

Therefore the signal $\varphi_{\text{GS}}(t_{3*}^{\text{GS}})$ is given by

$$\varphi_{\text{GS}}(t_{3*}^{\text{GS}}) = \Phi[I_{B_2}] - \Phi[I_{B_1}] = (\omega_{13}^* - \omega_{13})t_{3*}^{\text{GS}} + (\omega_{13} - \omega_{11})\tau_l + \omega_\uparrow\Delta t_{12} - \omega_\uparrow^*\Delta t_{12}^* + \omega_\downarrow\Delta t_{23} - \omega_\downarrow^*\Delta t_{23}^*. \tag{S-58}$$

For the signal $\varphi_{\text{SC}}(t_{2*}^{\text{SC}})$, at second order in ϵ we find

$$\omega_\uparrow\Delta t_{12} - \omega_\uparrow^*\Delta t_{12}^* = -\omega_0[\tau_l(1 + \mathfrak{d}_1)(\mathfrak{d}_2 - \mathfrak{d}_1) + (l\vec{\nu}_{12}\cdot\vec{\beta}_1/c + \hat{n}_{12}\cdot\vec{a}_1\tau_l L/c^2)] =: -\omega_0\tau_l\mathfrak{s}_\uparrow \tag{S-59}$$

where we used Eqs. (S-42) and (S-43) for the frequencies and Eq. (S-47) for the coordinate propagation time. Hence

$$\mathfrak{s}_\uparrow = (1 + \mathfrak{d}_1)(\mathfrak{d}_2 - \mathfrak{d}_1) + \vec{\beta}_1\cdot(\vec{\beta}_2 - \vec{\beta}_1) - \mathfrak{d}_1(\mathfrak{d}_2 - \mathfrak{d}_1) + \hat{n}_{12}\cdot\vec{a}_1 L/c^2 = (\mathfrak{d}_2 - \mathfrak{d}_1) + \vec{\beta}_1\cdot(\vec{\beta}_2 - \vec{\beta}_1) + \hat{n}_{12}\cdot\vec{a}_1 T/c. \tag{S-60}$$

For the signal $\varphi_{\text{GS}}(t_{3*}^{\text{GS}})$ we find the phase acquired during the upward propagation of the beams is the same as the above expression, and for the return trip

$$\omega_\downarrow\Delta t_{23} - \omega_\downarrow^*\Delta t_{23}^* = -\omega_0\tau_l(\mathfrak{s}_\uparrow - 2\mathfrak{s}_\downarrow), \tag{S-61}$$

where

$$\mathfrak{s}_\downarrow = \vec{\beta}_2\cdot(\vec{\beta}_2 - \vec{\beta}_1) + \hat{n}_{12}\cdot\vec{g}_2 T/c. \tag{S-62}$$

E. The signal

The useful information can be extracted from the signal

$$S := \varphi_{\text{SC}}(t_{2*}^{\text{SC}}) - \tfrac{1}{2}\varphi_{\text{GS}}(t_{3*}^{\text{GS}}) = S_{\text{beats}} + S_{\text{loop}} + S_{\text{space}}, \tag{S-63}$$

where for the ease of the analysis we identified three contributions. All three are of the same order of magnitude.

E.1 Beat contribution

At our level of precision the difference of the two beat terms will have time dependence only through slowly-varying changes in frequencies and accelerations, and therefore we can ignore the $\mathcal{O}(\epsilon^2)$ difference between the proper time on the satellite and on the ground. The beats difference is given by

$$S_{\text{beats}} := \varphi_{\text{SC}}^{\text{beat}}(t_{2*}^{\text{SC}}) - \tfrac{1}{2}\varphi_{\text{GS}}^{\text{beat}}(t_{3*}^{\text{GS}}) = \delta\omega_0(t_{2*}^{\text{SC}} - t_{3*}^{\text{GS}}) = -delta\omega_0 T \tag{S-64}$$

and substituting Eq. (S-40) gives

$$S_{\text{beats}} = \omega_0\tau_l\big((\vec{\beta}_2 - \vec{\beta}_1)^2 - (\mathfrak{d}_2 - \mathfrak{d}_1)^2 + L\hat{n}_{12}\cdot(\vec{g}_2 - \vec{a}_1)/c^2\big). \tag{S-65}$$

E.2 Delay loop contribution

The phase difference due to the beams propagation through delay loops on the satellite and on the ground also contain only terms of the second order in ϵ or higher. Indeed,

$$S_{\text{loop}} := (\omega_{12} - \tfrac{1}{2}\omega_{13} - \tfrac{1}{2}\omega_0)\tau_l =: \omega_0\tau_l(s_{\text{loop}}^{(1)} + s_{\text{loop}}^{(2)}). \tag{S-66}$$

The contribution

$$s_{\text{loop}}^{(1)} := -\tfrac{1}{2}\hat{n}_{12}\cdot(\vec{\beta}_2 - \vec{\beta}_1) + \tfrac{1}{2}\hat{n}_{23}\cdot(\vec{\beta}_3 - \vec{\beta}_2), \tag{S-67}$$

is built from the first order quantities, but due to the first-order equality of

$$-\hat{n}_{23}\cdot\vec{\beta}_3 = \hat{n}_{12}\cdot\vec{\beta}_1 = \mathfrak{d}_1, \qquad -\hat{n}_{23}\cdot\vec{\beta}_2 = \hat{n}_{12}\cdot\vec{\beta}_2 = \mathfrak{d}_2, \tag{S-68}$$

$s_{\text{loop}}^{(1)}$ is of the second order in ϵ. Substituting the leading order expansion of $\hat{n}_{23} = -\hat{n}_{12} + \epsilon\vec{\nu}$ and $\vec{v}_3 = \vec{v}_1 + 2L\epsilon\vec{a}_1/c$ we find

$$s_{\text{loop}}^{(1)} = \tfrac{1}{2}\big(\vec{\nu}\cdot(\vec{\beta}_1 - \vec{\beta}_2) - 2L\hat{n}_{12}\cdot\vec{a}_1/c^2\big). \tag{S-69}$$

Using Eq. (S-23) for $\vec{\nu}$, the above equation reduces to

$$s_{\text{loop}}^{(1)} = -\mathfrak{d}_1^2 + \mathfrak{d}_1\mathfrak{d}_2 + \beta_1^2 - \vec{\beta}_1\cdot\vec{\beta}_2 - T\hat{n}_{12}\cdot\vec{a}_1/c, \tag{S-70}$$

The term $S_{\text{loop}}^{(2)}$ is given by

$$s_{\text{loop}}^{(2)} = U_2 - U_1 + \tfrac{1}{2}\big((\hat{n}_{12}\cdot\vec{\beta}_1)^2 - (\hat{n}_{23}\cdot\vec{\beta}_2)^2 - \beta_1^2 + \beta_2^2$$
$$+ \hat{n}_{12}\cdot\vec{\beta}_2\,\hat{n}_{23}\cdot(\vec{\beta}_2 - \vec{\beta}_3) - \hat{n}_{12}\cdot\vec{\beta}_1(\hat{n}_{12}\cdot\vec{\beta}_2 + \hat{n}_{23}\cdot\vec{\beta}_2 - \hat{n}_{23}\cdot\vec{\beta}_3) + \hat{n}_{23}\cdot\vec{\beta}_2\,\hat{n}_{23}\cdot\vec{\beta}_3\big). \tag{S-71}$$

The above expression can be considerably simplified since we are interested only up to order ϵ^2 expression. Equation (S-71) reduces to

$$s_{\text{loop}}^{(2)} = U_2 - U_1 + \tfrac{1}{2}\beta_2^2 - \tfrac{1}{2}\beta_1^2 + \mathfrak{d}_1\mathfrak{d}_2 - \mathfrak{d}_2^2, \tag{S-72}$$

finally giving

$$S_{\text{loop}} = \omega_0\tau_l(U_2 - U_1 + \tfrac{1}{2}(\vec{\beta}_1 - \vec{\beta}_2)^2 - (\mathfrak{d}_1 - \mathfrak{d}_2)^2 - T\hat{n}_{12}\cdot\vec{a}_1/c). \tag{S-73}$$

E.3 Propagation difference

The phase difference due to the difference in paths the beams propagate along is

$$S_{\text{space}} = -\omega_0\tau_l\big(\mathfrak{s}_\uparrow - \tfrac{1}{2}(2\mathfrak{s}_\uparrow - 2\mathfrak{s}_\downarrow)\big) = -\omega_0\tau_l\mathfrak{s}_\downarrow, \tag{S-74}$$

and by using Eq. (S-62),

$$S_{\text{space}} = -\omega_0\tau_l\left[\vec{\beta}_2\cdot(\vec{\beta}_2 - \vec{\beta}_1) + \hat{n}_{12}\cdot\vec{g}_2 T/c\right] \tag{S-75}$$

E.4 Final expression

From a phenomenological point of view, the possible violation of LPI is parametrized by

$$g_{00} = -1 + (1+\alpha)2U + \dots , \tag{S-76}$$

leading, as an example, to Eq. (1).

For our proposal, putting Eqs. (S-65), (S-73) and (S-75) into (S-63), the final expression for the signal from which a bound on α will be obtained is

$$S = \omega_0 \tau_l \left[U_2 - U_1 + \frac{3}{2}(\vec{\beta}_1 - \vec{\beta}_2)^2 - \vec{\beta}_2 \cdot (\vec{\beta}_2 - \vec{\beta}_1) - 2(\mathfrak{d}_1 - \mathfrak{d}_2)^2 - 2T\hat{n}_{12} \cdot \vec{a}_1/c \right] , \tag{S-77}$$

which, by taking into account Eq. (S-76), finally gives Eq. (14) of the main text.

F. Unequal delay times

It is impossible for the two delay lines to be perfectly identical. We define the relative difference in the proper propagation times δ_l as

$$\delta_l := \frac{\tau_l^{\mathrm{SC}} - \tau_l^{\mathrm{GS}}}{\tau_l^{\mathrm{GS}}} := \frac{\Delta \tau_l}{\tau_l^{\mathrm{GS}}} , \tag{S-78}$$

which can be made suitably small and in the following we assume that $\delta_l < \epsilon$. The delay time difference affects only the signal φ_{SC}. In principle, it affects both the delay phase and the beat term, due to the additional contribution to the arrival time mismatch. In this case the latter quantity becomes

$$\Delta T = \frac{L^* - L}{c} + \tau_l \delta_l = \tau_l(\mathfrak{d}_2 - \mathfrak{d}_1 + \delta_l), \tag{S-79}$$

which at our level of precision still gives the beat term $(\omega_{12}^* - \omega_{12})t_{2*}^{\mathrm{SC}}$. On the other hand, the delay line contribution provides a constant phase offset and the additional term of the $\epsilon\delta_l$ that results from the first order Doppler effect,

$$\Delta\varphi_{\mathrm{SC}} = \omega_{12}\tau_l\delta_l = \omega_0\big(1 + (\mathfrak{d}_1 - \mathfrak{d}_2)\big)\tau_l\delta_l . \tag{S-80}$$

Hence

$$\Delta S/(\omega_0\tau_l) = \delta_l + (\mathfrak{d}_1 - \mathfrak{d}_2)\delta_l. \tag{S-81}$$